NANO LETTERS

2007
Vol. 7, No. 9
2627−2632

Uniaxial Alignment of Nanoconfined Columnar Mesophases

Pierre-Olivier Mouthuy,*,† Sorin Melinte,† Yves H. Geerts,‡ and Alain M. Jonas†

Cermin, Université Catholique de Louvain, 1348 Louvain-la-Neuve, Belgium, and Laboratory of Polymer Chemistry, CP206/1, Université Libre de Bruxelles, Boulevard du Triomphe, 1050 Bruxelles, Belgium

Received April 28, 2007; Revised Manuscript Received July 7, 2007

ABSTRACT

By confining discotic phthalocyanines in a network of crisscrossed nanogrooves, we obtain a uniaxial alignment of the columnar mesophase. The alignment process is based on the anisotropy of interface tension between the mesophase and the nanogrooves' walls. Preferential mesophase alignment results from this nonhomogeneity combined with the anisotropy of the network cell dimensions. A simple model is proposed to explain the experimental observations.

Liquid-crystalline (LC) π-conjugated molecules are promising materials for organic electronics. Their intrinsic electronic properties combined with their trend to form large ordered domains make them potential candidates for semiconducting devices including transistors and solar cells.[1] For applications, advances should be made into a series of critical issues such as long-range order, level of impurities, and fabrication of reliable contacts and interfaces. Given the anisotropy of properties of LC phases, controlling the orientation and the uniformity of the molecular packing is crucial. This alignment is of paramount importance for discotic molecules stacking into columnar phases, as charge transport occurs along the columnar axis.[2] Because these molecules consist of a π-conjugated rigid core surrounded by an insulating aliphatic crown, each column forms an individual semiconducting nanowire.[3] Skillful scaling down of the orientational control to the nanometer range, and ultimately to single columns, would permit a high density of organic nanowires integration.

Several techniques for aligning columnar mesophases in homogeneous films have been investigated[4] by infrared polarized laser,[5] dip-coating,[6] epitaxial layers,[7] self-assembled monolayers,[8] and magnetic field[9] and chemical grafting.[10,11] In addition, organic nanowires made of a limited number of aligned columns have been realized in the nanopores of an alumina matrix.[12] However, the confined planar uniaxial alignment is more challenging to accomplish and has not been achieved so far. Here, we present a novel alignment method for producing a bidimensional network of oriented LC phthalocyanines. The method relies on controlling the anisotropic interfacial tension of discotic columns: by properly designing the template geometry, the alignment of columns is forced in specific directions. A simple model is put forward to interpret the results. This orientation method opens perspectives for the rational engineering of arrays of nanowires of liquid-crystalline organic semiconductors.

The molecule used in this study is a peritetrasubstituted phthalocyanine (Pc, Figure 1a). This LC compound presents a columnar mesophase at room temperature and melts above 450 K.[13] The charge transport along the columns was studied previously from both theoretical[3] and experimental[14] points of view. Time-of-flight transient photoconductivity measurements on homeotropically aligned samples provided 1.10^{-3} $cm^2/V\cdot s$ as typical mobility, comparable to other discotics such as hexabenzocoronene.

Thin films of Pc exhibit planar alignment of the columns after annealing (Figure 1b). On the other hand, the columns show homeotropic alignment when annealed between two glass plates[15] (Figure 1c). In the sequel, the orientation of columns perpendicular and parallel to an interface will be signaled by superscripts $\perp$ and $\parallel$, respectively, with the subscript indicating the interface type. The above observations can be rewritten in terms of interfacial tensions as $\gamma^{\parallel}_{Pc/air} < \gamma^{\perp}_{Pc/air}$ and $\gamma^{\perp}_{Pc/glass} < \gamma^{\parallel}_{Pc/glass}$.[16]

An interesting circumstance occurs when Pc's are introduced in open nanogrooves (Figure 1d), as four interfaces have to be considered, offering increased opportunities to tune the mesophase alignment. A set of parallel grooves of 200 nm width have been fabricated by e-beam lithography (EBL) using a 40 nm thick poly(methylmethacrylate) (PMMA) mask followed by a 30 nm deep etching of the underlying oxidized silicon wafer. The grooves were then filled by spin-coating the molecules from a hexadecane solution (see

* Corresponding author. E-mail: mouthuy@dice.ucl.ac.be.
† Cermin, Université Catholique de Louvain.
‡ Laboratory of Polymer Chemistry, CP206/1, Université Libre de Bruxelles.

10.1021/nl0710102 CCC: $37.00
Published on Web 08/09/2007

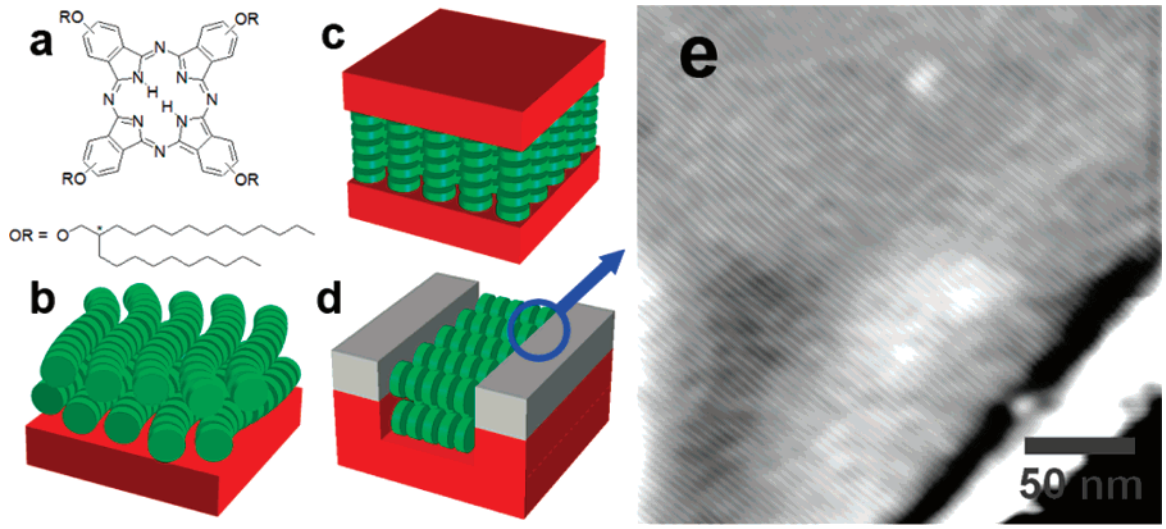

Figure 1. (a) Chemical structure of Pc. (b−d) Schematic drawings of the alignment of Pc columns exposed to air (b), sandwiched between two solid surfaces (c), or in a nanogroove (d) as shown in the AFM phase image taken at its edge (e).

Supporting Information). After flash-annealing and removal of the mask, polarized optical microscopy in reflection (POM) showed preferential alignment of the molecules with respect to the grooves. Because of the 90° rotational symmetry of POM images, the direction of the columnar axis could not be decided unambiguously. Atomic force microscopy in tapping mode (AFM) was used (Figure 1e) to show that the columns adopt a planar configuration, with their axis perpendicular to the vertical walls of the grooves (Figure 1d). This orientation satisfies the energetic requirements at the two vertical walls and at the interface with air. However, for transport along the nanogrooves, this stable configuration would be unfavorable because the molecular stacks are perpendicular to the grooves' walls.

To force the alignment to occur in the proper direction, we have added a second set of orienting nanogrooves with respect to the first one. As the sets of grooves are perpendicular to each other, they deliver conflicting orientation instructions to the molecules. Therefore, the system may either attain a randomized equilibrium state, with orientational constraints being respected at the local scale but with no long-range order, or settle in a frustrated state displaying a long-range preferred alignment, with only one set of orientational instructions being met. The selection between these two possibilities depends on many parameters, among which are the bending modulus of the columns, the energy cost of grain boundaries, and the dimensions of the two sets of grooves. To elucidate the role of these dimensions, we have adopted a high-throughput screening approach by fabricating in the $\vec{x}_1$ direction a set of parallel grooves of constant width W_1 and of increasing period $L_1(n) = L_{1,0} + n\Delta L_1$ for the nth line. By tracing a second similar set at 90° to the previous one, in the $\vec{x}_2$ direction, a network with varying cell dimensions is obtained (Figure 2a). Experimental parameters are summarized in Table 1. This network is filled with Pc as described above, and the AFM result is shown in Figure 2a. In the upper left corner of the network, where $L_2 > L_1$ (Figure 2b,c), columns parallel to $\vec{x}_1$ are observed in high-resolution phase images. Likewise, in the lower right corner, where $L_1 > L_2$ (Figure 2d,e), the columns are aligned parallel to $\vec{x}_2$. Considering the cells of the network boxed in Figure 2b,d, it appears that, in both cases, this uniform alignment of the columns is imposed by the longest wall. The rectangular cell of the network is depicted in Figure 2f.

To screen orientational changes over the whole network, the sample is inserted between crossed polarizers, with $\vec{x}_1$ along the bisector of their axes. The resulting POM image is presented in the left panel of Figure 3. It could be decomposed in three zones. In region a, the reflectivity varies strongly. The corresponding variation in orientation is due to the fluctuation of the contact area between the mesophase and the nanogrooves walls. The Pc network thickness is indeed irregular and lower in this region than elsewhere, as displayed in Figure 2a.[17] A detailed analysis of this region is complex and will not be done here. The region b displays a strong reflectivity that corresponds to homogeneous alignment of the columns in directions $\vec{x}_1$ or $\vec{x}_2$, as illustrated by AFM. The black zones around the diagonal mark the transition region for which the average orientation is the bisector of $(\vec{x}_1, \vec{x}_2)$. The extent of this zone is quite narrow. Upon increasing (L_1, L_2), the transition region spreads. This corresponds to region c in Figure 3, showing a patchwork of small domains apparently randomly oriented. It is remarkable that, even in this disordered region, most domains actually align either along $\vec{x}_1$ or along $\vec{x}_2$ and refrain from choosing intermediary states, except at boundaries between domains of different orientations. Among all the possible alignment directions, these states are consequently the most stable.

The above observations imply that the Pc columns within the zones b and c of the network (Figure 3) are mostly parallel to $\vec{x}_1$ or $\vec{x}_2$. To analyze our data in light of a thermodynamic/kinetic model, we thus denote as "state i" the case of columns aligned perpendicular to $\vec{x}_i$. This limitation of column alignment to only two uniaxial states allows us to neglect all bending terms in mesophase free

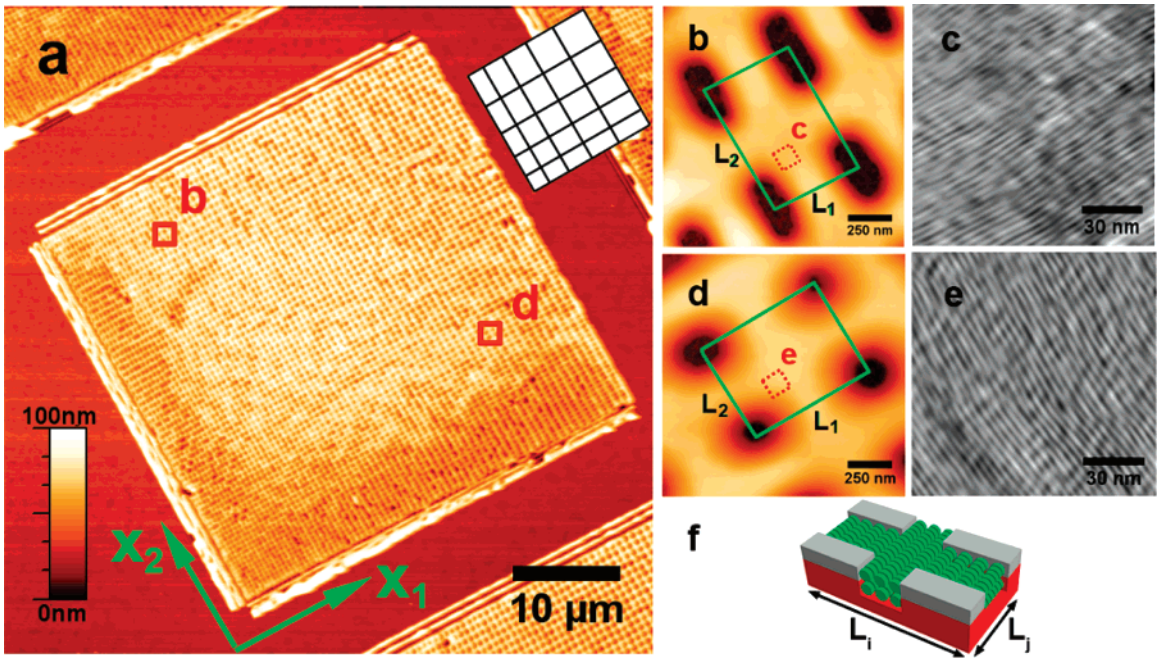

Figure 2. (a) AFM topography image of the 40 μm × 40 μm Pc network used to screen column alignment. The periods of the grooves increases progressively, as shown schematically in the inset. (b,d) AFM topographic zoom on the region marked in (a). The column alignment is observed in the corresponding AFM phase images shown in (c) and (e). (f) Schematic drawing of the alignment of columns in a rectangular cell of the network.

Table 1. Main Geometrical Parameters of the Studied Networks: Width (W), Period Increment (ΔL), Minimal Period (L_0), and Maximal Period (L_{max})[a]

figures	$W_1 = W_2$, nm	$\Delta L_1 = \Delta L_2$, nm	$L_{1,0} = L_{2,0}$, nm	$L_{1,max} = L_{2,max}$, nm
2,3	200	5	400 ($x_1 = x_2 = 0$ μm)	800 ($x_1 = x_2 = 40$ μm)
4			475 ($x_1 = x_2 = 7.5$ μm)	800 ($x_1 = x_2 = 40$ μm)

[a] The coordinates are explicited for POM images shown in Figures 3 and 4.

energy[18] and consider only surface energies. Because the isotropic/mesophase transition is a first-order phase transition, it happens through a nucleation and growth process.[19] For simplicity, we suppose that all domains are nucleating at the same time, are equidistant from each other, and have the same growth rate during the experiment. Under these circumstances, the system in which energy should be minimized is the ordered domain of mesophase growing in the isotropic melt.[16] We further assume that the states are univocally defined all over the domain. Considering that the interfacial tension of ordered mesophase/isotropic melt boundaries is negligible as compared to the tension between an ordered domain and groove walls,[16] the difference of energy between states i and j of a growing domain reads as:

$$\Delta E_{ij} = t(l_i - l_j) * (\gamma^{\perp}_{Pc/w} - \gamma^{||}_{Pc/w}), \qquad i \neq j \in \{1,2\} \qquad (1)$$

where t is the depth of the grooves, $\gamma_{Pc/w}$ is the average interfacial tension between sidewalls and the columnar mesophase, l_i and l_j are the summed lengths of the walls parallel to $\vec{x}_i$ and $\vec{x}_j$, respectively, in contact with the growing domain. Gibbs' equilibrium equations give the probability for the growing domain to be in state i:

$$P_i = \left[1 + \exp\left(\frac{\Delta E_{ij}}{k_B T}\right)\right]^{-1}, i \neq j \in \{1,2\} \qquad (2)$$

where k_B is the Boltzmann constant and $T = 450$ K, i.e., the isotropic/mesophase transition temperature.

The ordering process is a dynamic phenomenon that spreads over the experimental time t_{exp}. Consider the two states of a growing domain, as shown in Figure 3d,e. The average relaxation time from state i to state j is of the form:

$$\tau_{i\to j} \propto \exp\left(\frac{\Delta E^*_{i\to j}}{k_B T}\right), \qquad i \neq j \in \{1,2\} \qquad (3)$$

where $\Delta E^*_{i\to j}$ is the height of the energy barrier seen when moving from i to j (see Figure 3e). For short times elapsed from nucleation, and therefore small diameter, this barrier is low and the system can easily change state. With time, the ordered domain size increases[20] and so does ΔE_{ij} ($\Delta E_{ij}(\beta) > \Delta E_{ij}(\alpha)$ in Figure 3d,e). This should force the system to reach equilibrium if $\Delta E^*_{i\to j}$ remains small. However, at the end of the experiment, states i are still observed in regions where the system should adopt state j. These metastable states are localized nearby the diagonal in region b of Figure 3 and stay unchanged for days. This implies that, during our experiment, $\tau_{i\to j}$ becomes too large compared to t_{exp}. From a given time t_{limit}, corresponding to a mean diameter d_{limit}, the growing domain cannot reorient anymore and its orientation is frozen in the last reached state. The

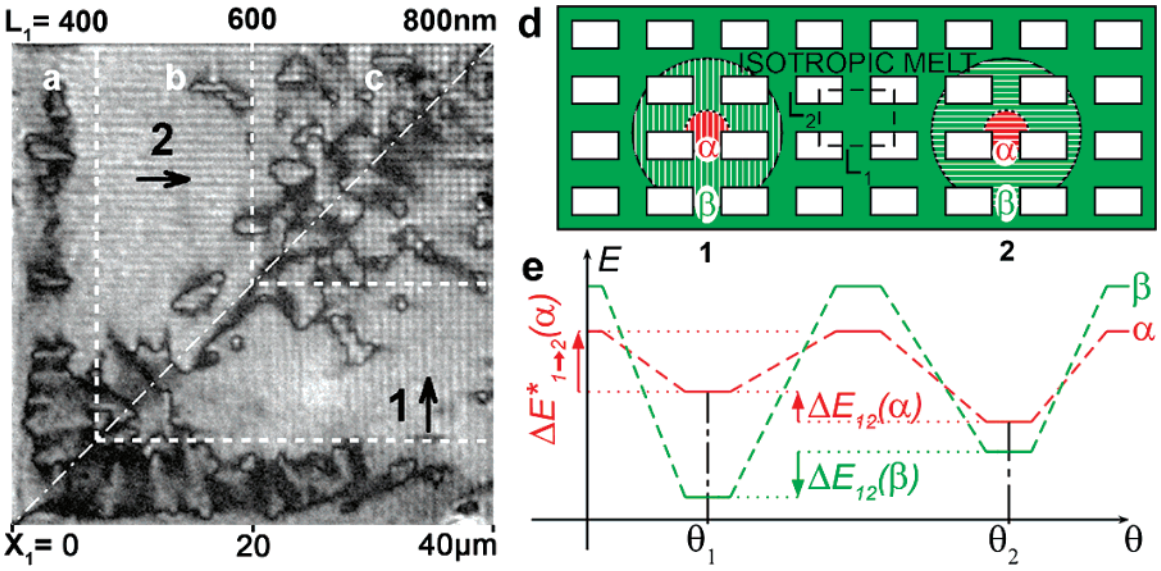

Figure 3. Left panel: POM image of the network, split in three parts: (a) a region of variable thickness, (b) a region of constant thickness and strong alignment, and (c) a region of constant thickness and random alignment of columns along $\vec{x}_1$ or $\vec{x}_2$. Right panel: (d) schematic drawing of growing domains in a network of fixed dimensions in states 1 and 2 and (e) schematic diagram of the energy vs alignment angle θ of the columns in the growing domain for two stages of growth α and β. The dashed curve is drawn as qualitative support to the eye.

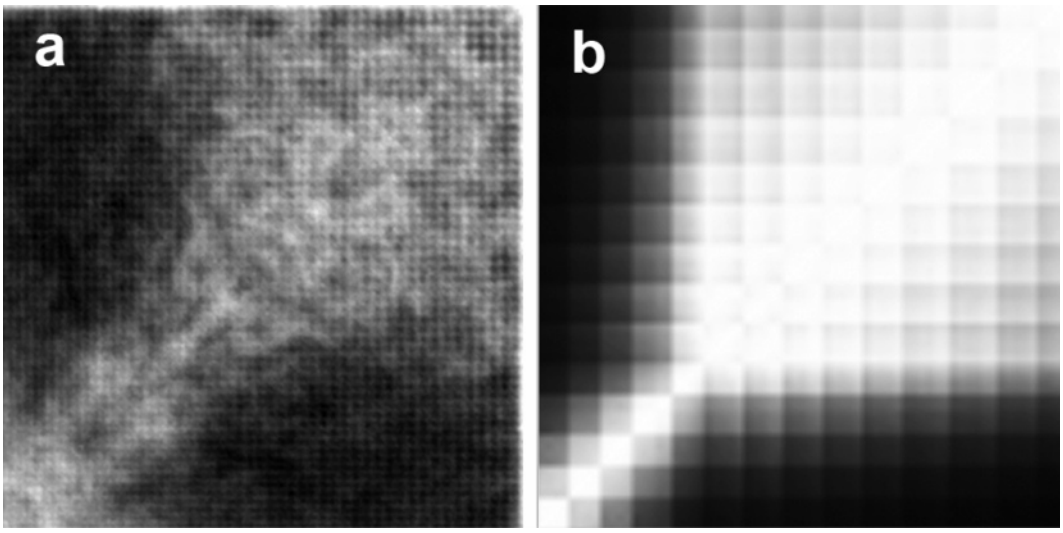

Figure 4. Comparison between experiment and a simple theoretical model for regions (b,c) displayed in the left pannel of Figure 3. (a) Folded average of 8 gray scale inverted POM images. (b) The P_{12} fit (see text).

domain then grows in this orientation until generalized coalescence.

The idea of time-dependent reorganization of columns within a growing domain is not new.[16] In fact, it was suggested that viscosity is a key factor controlling the kinetics. In our model, it should dictate the reorganization time and the energy barrier. As both the number and the length of the columns increase when the domain grows, viscosity should gradually hinder the change of state, favoring the formation of metastable domains. This is supported by our experimental results, including the ones presented in Supporting Information. Therefore, we just need to consider the domains at t_{limit} to predict their orientation. If the system is then treated as quasistatic, the probability distribution for states is given by Gibbs' equation.

If L_{limit} represents the maximal size of a squared network cell encompassed by a circular domain of diameter d_{limit}, it is now possible to explain the shape of the transition region in Figure 3b,c. For L_1, $L_2 < L_{limit}$, the growing domain at t_{limit} at least embraces one cell (case β of Figure 3d). In this regime, while the interfacial energy weakly depends on the domain center position, the probability for state i is globally given by P_i and rapidly decreases for growing values of $l_i - l_j$ (eqs 1 and 2). Hence, the transition between the two states is rather sharp, as shown in region b of Figure 3, and the uniaxial alignment results from the anisotropy of the network cell dimensions. When L_1, $L_2 > L_{limit}$ (case α of Figure 3d), the growing domain at orientational freezing does not encompass an entire cell and thus cannot balance energies with respect to the cell dimensions. The orientation is

imposed by the nearest wall and the domain center position within the cell is determinant. The probability for state i is then directly linked to the probability for the domain to nucleate close to a wall parallel to $\vec{x}_i$. If we suppose that nucleation can equiprobably occur all over the LC interfaces, $P_i \approx 0.5$. This corresponds to region c of Figure 3.

To consolidate our analysis, we compute the folded average of the POM inverted images of eight Pc networks (Figure 4a). The value of L_{limit} from which the loss of orientation starts to diverge from the diagonal is around 600 nm (see Table 1). As mentioned above, POM images do not provide the absolute orientation of the Pc columns. What can safely be extracted is improper alignment with respect to either $\vec{x}_1$ or $\vec{x}_2$, which appears black in Figure 3.[21] As only two possible states were defined in our simple model, no energy nor probability can be associated to improperly aligned regions. Nevertheless, it is realistic to assume that the probability of finding any intermediary state is proportional to the probability to find both states 1 and 2: $P_{12} = P_1 \times P_2$. This latter probability is easily calculable and allows us to estimate driving parameters for the alignment process. We thus have modeled the problem by assuming that the growing domains adopt a perfect circular shape. For given values of (L_1, L_2), we distribute n points equally spaced over the cell area. Then, according to eq 1, we calculate the ΔE_{ij} of domains centered on each of these points in a homogeneous network of constant cell dimensions (L_1, L_2). Averaging ΔE_{ij} on all points, we then extract the probability for state i for local values of the networks parameters (L_1, L_2). Repeating this for all experimental values (L_1, L_2) provides the probability distribution for state i over the whole experimental network. Parameters can be determined by fitting the image shown in Figure 4a: $d_{\text{limit}} = 950$ nm,[22] $|\gamma^{\perp}_{\text{Pc/w}} - \gamma^{\parallel}_{\text{Pc/w}}|\, t = 6.10^{-14}$ (J/m). With $t = 70$ nm, we get $|\gamma^{\perp}_{\text{Pc/w}} - \gamma^{\parallel}_{\text{Pc/w}}| = 10^{-6}$ (J/m^2). This lies within the limit $|\gamma^{\perp}_{\text{Pc/w}} - \gamma^{\parallel}_{\text{Pc/w}}| < 10^{-4}$ (J/m^2) proposed elsewhere,[16] indicating that our model is quantitatively reasonable. The image computed with these parameters is shown in Figure 4b. We therefore conclude that this simple model captures the essential physics of the preferential alignment observed in our experiments.[23]

In conclusion, we have developed a method for aligning Pc columns in specific directions, making use of a bidimensional network of grooves. We have shown how interfacial tensions and domain growth control the orientation and proposed a model that successfully reproduces the salient features of our experimental results. Our alignment method is general, provided that the discotic liquid crystal satisfies a set of conditions corresponding to both thermodynamic and kinetic aspects. First, the gain of energy due to alignment should be dominant compared to the thermal energy: $\Delta E_{ij} \gg k_B T$. Although $|\gamma^{\perp}_{\text{Pc/w}} - \gamma^{\parallel}_{\text{Pc/w}}|$ is fixed by the very nature of the molecules considered, ΔE_{ij} can be tuned by choosing the depth and the materials of the grooves walls, as well as optimizing the network anisotropy $L_i - L_j$. Second, the growing domain (at orientational freezing) must have a diameter larger than the dimensions of the network cell: $L_{\text{limit}} > (L_1, L_2)$. While d_{limit} should be adjustable by changing the cooling rate, we expect that the available range for L_1, L_2 is limited to submicrometer dimensions. This method opens the route to the rational design of discotics nanowires, where the alignment strength can be tuned at will and remains permanent because interfacial forces never vanish.

Acknowledgment. We are grateful to Prof. P. Ruelle, Prof. J.-P. Ryckaert, Prof. M. Baus, T. De Vos, and R. Comblen for discussions. We thank the DICE clean room team, P. Lipnik, S. Derclaye, Prof. B. Nysten, Prof. R. Lazzaroni, and P. Viville for help with experiments. Financial support was provided by ARC-Dynanomove, ARC-Nanomol, RW Nanotic-Feeling, and Cite and IUAP FS2. P.-O. Mouthuy is a research fellow of the Belgian FNRS.

Supporting Information Available: Experimental materials, techniques, methods, simulation details, and additional experiments. This material is available free of charge via the Internet at http://pubs.acs.org.

References

(1) Takatoh, K.; Hasegawa, M.; Koden, M.; Itoh, N.; Hasegawa, R.; Sakamoto, M. *Alignment Technologies and Applications of Liquid Crystal Devices;* Gray, G. W., Goodby, J. W., Fukuda, A., Eds.; Taylor & Francis: New York, 2005.
(2) Ohta, K.; Hatsusaka, K.; Sugibayashi, M.; Ariyoshi, M.; Ban, K.; Maeda, F.; Naito, R.; Nishizawa, K.; van de Craats, A. M.; Warman, J. M. *Mol. Cryst. Liq. Cryst.* **2003**, *25*, 397.
(3) Tant, J.; Geerts, Y. H.; Lehmann, M.; De Cupere, V.; Zucchi, G.; Laursen, B. W.; Bjornholm, T.; Lemaur, V.; Marcq, V.; Burquel, A.; Hennebicq, E.; Gardebien, F.; Viville, P.; Beljonne, D.; Lazzaroni, R.; Cornil, J. *J. Phys. Chem. B* **2005**, *109*, 20315.
(4) Eichhorn, S. H.; Adavelli, A.; Li, H. S.; Fox, N. *Mol. Cryst. Liq. Cryst.* **2003**, *397*, 47.
(5) Monobe, H.; Awazu, K.; Shimizu, Y. *Adv. Mater.* **2006**, *18*, 607.
(6) Miskiewicz, P.; Rybak, A.; Jung, J.; Glowacki, I.; Ulanski, J.; Geerts, Y.; Watson, M.; Müllen, K. *Synth. Met.* **2003**, *137*, 905.
(7) van de Craats, A. M.; Stutzmann, N.; Bunk, O.; Nielsen, M. M.; Watson, M.; Müllen, K.; Chanzy, H. D.; Sirringhaus, H.; Friend, R. H. *Adv. Mater.* **2003**, *15*, 495.
(8) Monobe, H.; Terasawa, N.; Kiyohara, K.; Shimizu, Y.; Azehara, H.; Nakasa, A.; Fujihira, M. *Mol. Cryst. Liq. Cryst.* **2004**, *412*, 229.
(9) Shklyarevskiy, I. O.; Jonckheijm, P.; Stutzmann, N.; Wasserberg, D.; Wondergem, H. J.; Christianen, P. C. M.; Schenning, A. P. H. J.; De Leeuw, D. M.; Tomovic, Z.; Wu, J.; Müllen, K.; Maan, J. C. *J. Am. Chem. Soc.* **2005**, *127*, 2825.
(10) Wang, Z.; Watson, M. D.; Wu, J.; Müllen, K. *Chem. Commun.* **2004**, *3*, 336.
(11) Thunemann, A. F.; Ruppelt, D.; Burger, C.; Müllen, K. *J. Mater. Chem.* **2000**, *10*, 1325.
(12) Steinhart, M.; Zimmermann, S.; Goring, P.; Schaper, A. K.; Gosele, U.; Weder, C.; Wendorff, J. H. *Nano Lett.* **2005**, *5*, 429.
(13) Gearba, R. I.; Bondar, A. I.; Goderis, B.; Bras, W.; Ivanov, D. A. *Chem. Mater.* **2005**, *17*, 4273.
(14) Deibel, C.; Janssen, D.; Heremans, P.; De Cupere, V.; Geerts, Y. H.; Benkhedir, M. L.; Adriaenssens, G. J. *Org. Electron.* **2006**, *7*, 495.
(15) De Cupere, V.; Tant, J.; Viville, P.; Lazzaroni, R.; Osikowicz, W.; Salaneck, W. R.; Geerts, Y. H. *Langmuir* **2006**, *22*, 7798.
(16) Grelet, E.; Bock, H. *Europhys. Lett.* **2006,** *73*, 712.
(17) Because of higher EBL proximity effects, the width of the two grooves sets is not constant here. The liquid level is thus unequally redistributed following Laplace pressure during its annealing in the isotropic phase.
(18) de Gennes, P. G.; Prost, J. *The Physics of Liquid Crystals*; Birman, J., Edwards, L., Smith, C. H., Rees, M., Eds.; Oxford University Press: New York, 1993.
(19) Markov, I. In *Crystal Growth and Characterization of Advanced Materials*; Christensen, A. N., Leccabue, F., Paorici, C., Vigil; O., Eds.; World Scientific: Singapore, 1988.
(20) Coalescence of domains is here simply treated as a way of growth of the system.

(21) Such regions are supposed to appear through the coalescence of two growing domains frozen in opposite states.

(22) As expected, d_{limit} roughly corresponds to $\sqrt{2}\ L_{limit}$, i.e., the diameter of a circular domain entirely encompassing a squared cell of dimensions L_{limit}. Note that if orientational freezing is due to generalized coalescence, d_{limit} represents the mean distance between germs centers at coalescence.

(23) We note that the thickness over which preferential order is kept may be lost near the bottom of the grooves. In addition, we have not taken into account the distribution of domain sizes and the possible preferential nucleation of domains at edges and corners.

NL0710102